Purinergic receptor P2X7 regulates interleukin-1α mediated inflammation in chronic kidney disease in a reactive oxygen species-dependent manner

see commentary on page 389

OPEN

Maryam Amini[1], Janina Frisch[2,3,4], Priska Jost[1], Tamim Sarakpi[5,6], Simina-Ramona Selejan[7], Ellen Becker[8], Alexander Sellier[8], Jutta Engel[2], Michael Böhm[7], Mathias Hohl[7], Heidi Noels[9], Christoph Maack[10], Stefan Schunk[8], Leticia Prates Roma[2,3,4], Barbara A. Niemeyer[1], Thimoteus Speer[5,6] and Dalia Alansary[1]

[1]Molecular Biophysics, Saarland University, Homburg, Germany; [2]Institute of Biophysics, Saarland University, Homburg, Germany; [3]Center of Human and Molecular Biology (ZHMB), Saarland University, Homburg, Germany; [4]Center for Gender-Specific Biology and Medicine (CGBM), Saarland University, Homburg, Germany; [5]Department of Internal Medicine 4, Nephrology, Goethe University Frankfurt, Frankfurt, Germany; [6]Goethe University Frankfurt, Else Kröner Fresenius Center for Nephrological Research, Frankfurt, Germany; [7]Department of Internal Medicine III, Cardiology, Angiology and Intensive Care Medicine, Saarland University, Homburg, Germany; [8]Department of Internal Medicine IV, Nephrology and Hypertension, Saarland University, Homburg, Germany; [9]Institute for Molecular Cardiovascular Research (IMCAR), University Hospital RWTH Aachen, Aachen, Germany; and [10]Medical Clinic 1, University Clinic Würzburg, Würzburg, Germany

Onset, progression and cardiovascular outcome of chronic kidney disease (CKD) are influenced by the concomitant sterile inflammation. The pro-inflammatory cytokine family interleukin (IL)-1 is crucial in CKD with the key alarmin IL-1α playing an additional role as an adhesion molecule that facilitates immune cell tissue infiltration and consequently inflammation. Here, we investigate calcium ion and reactive oxygen species (ROS)-dependent regulation of different aspects of IL-1α-mediated inflammation. We show that human CKD monocytes exhibit altered purinergic calcium ion signatures. Monocyte IL-1α release was reduced when inhibiting P2X7, and to a lesser extent P2X4, two ATP-receptors that were found upregulated compared to monocytes from healthy people. In murine CKD models, deleting P2X7 ($P2X7^{-/-}$) abolished IL-1α release but increased IL-1α surface presentation by bone marrow derived macrophages and impaired immune cell infiltration of the kidney without protecting kidney function. In contrast, immune cell infiltration into injured wild type and $P2X7^{-/-}$ hearts was comparable in a myocardial infarction model, independent of previous kidney injury. Both the chimeric mouse line harboring $P2X7^{-/-}$ immune cells in wild type recipient mice, and the inversely designed chimeric line showed less acute inflammation. However, only the chimera harboring $P2X7^{-/-}$ immune cells showed a striking resistance against injury-induced cardiac remodeling. Mechanistically, ROS measurements reveal P2X7-induced mitochondrial ROS as an essential factor for IL-1α release by monocytes. Our studies uncover a dual role of P2X7 in regulating IL-1α biogenesis with consequences for inflammation and inflammation-induced deleterious cardiac remodeling that may determine clinical outcomes in CKD therapies.

Correspondence: *Dalia Alansary, Molecular Biophysics, Saarland University Hospital and Saarland University Faculty of Medicine, Kirrbergerstrasse 100, CIPMM Building 48, 66421 Homburg, Germany. E-mail: dalia.alansary@uks.eu*

Received 24 October 2023; revised 11 October 2024; accepted 17 October 2024; published online 20 November 2024

Kidney International (2025) **107,** 457–475; https://doi.org/10.1016/j.kint.2024.10.024

KEYWORDS: calcium; chronic kidney disease; cytokines; inflammation

Translational Statement

P2X7 is a Ca^{2+} permeable ionotropic purinergic receptor. Although it is known that P2X7 regulates the release of interleukin (IL)-1β, its role in regulating IL-1α biogenesis is largely unknown. We show that activating P2X7 results in mitochondrial reactive oxygen species production, which, in turn, is essential for IL-1α release. Importantly, genetic ablation of P2X7 is protective against chronic immune cell infiltration of the myocardium but not in the acute phase of cardiac injury. Strong cardiac protection is observed, however, in the chronic phase of heart injury, pointing to involvement of P2X7 in cardiac remodeling. Our findings draw the attention to a potential dual role of P2X7 in regulating inflammation and provide important considerations for clinical application of P2X7 antagonists in inflammatory diseases.

Chronic kidney disease (CKD) represent a significant worldwide health issue negatively impacting the quality of life.[1–4] Clinical manifestations of CKD are often complicated by comorbidities, including diabetes, making it exceedingly challenging to predict the risk of development of secondary morbidities, such as cardiovascular diseases (CVDs). Inflammation significantly shapes CKD progression

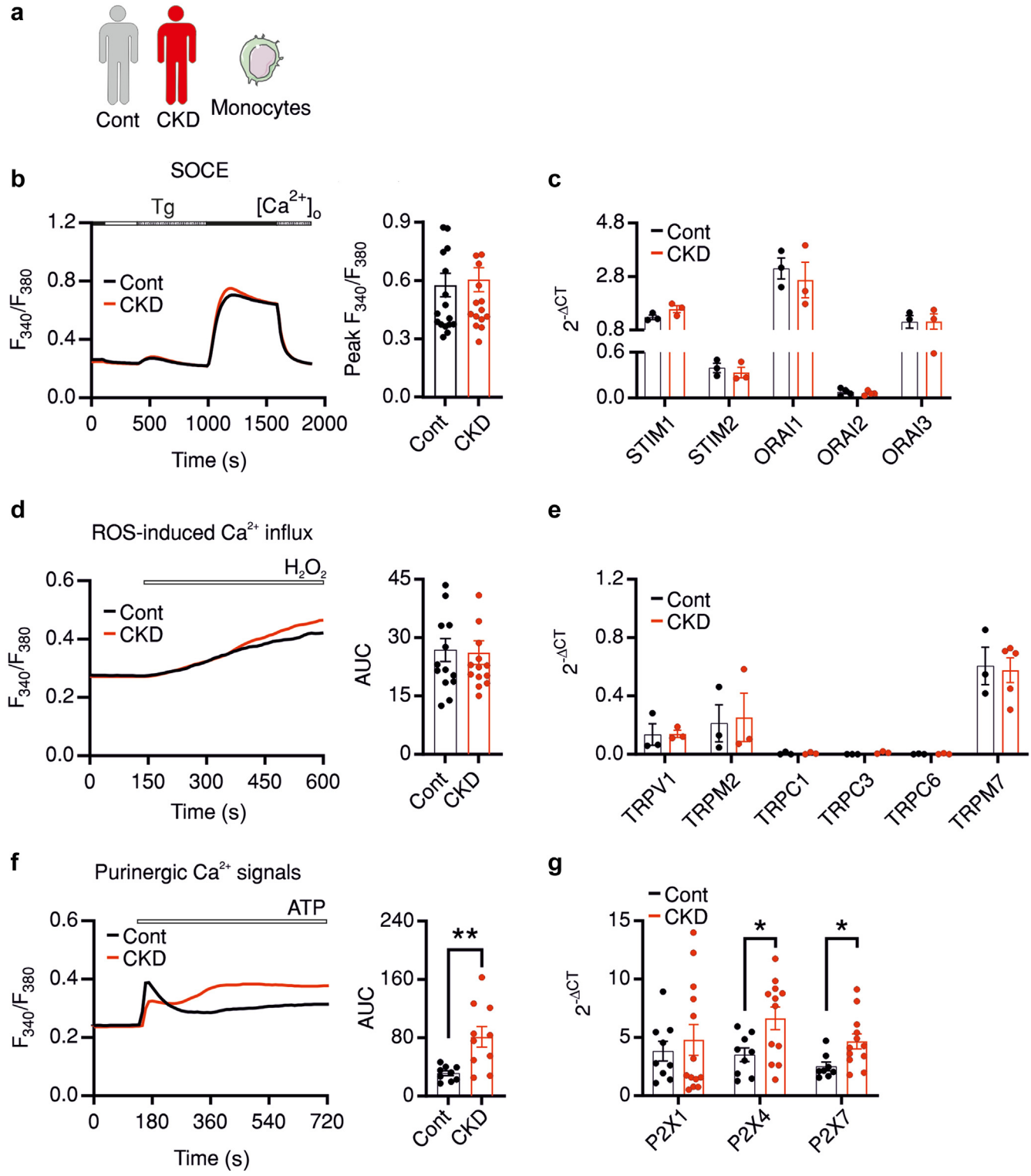

Figure 1 | Chronic kidney disease (CKD)–derived monocytes show altered purinergic Ca^{2+} signatures. (**a**) Human $CD14^{+}$ monocytes were isolated from healthy control (Cont) individuals (black) or patients with CKD (red) and loaded with 1 μM acetoxymethyl ester AM for (**b,d,f**) measurement of $[Ca^{2+}]_i$ or for (**c,e,g**) quantitative reverse transcription–polymerase chain reaction (RT-PCR) analysis using primers listed in Supplementary Tables S2 and S3. (**b**) Average traces showing changes of fluorescence ratio at 340 to 380 nm (F340/F380) over time in response to changes of extracellular solutions containing 0.5 mM $[Ca^{2+}]_o$ (black bar) or Ca^{2+} free external solution with or without 1 μM thapsigargin (Tg). The right panel represents quantification of maximal Ca^{2+} influx indicated by peak change of F340/F380. (**c**) Quantitative RT-PCR analysis of store-operated Ca^{2+} entry (SOCE) components expression in control or CKD monocytes. (**d**) Average traces showing changes of F340/F380 over time in response to application of 1 mM H_2O_2 and corresponding quantification of area under the response curve (AUC) measured in control or CKD monocytes. (**e**) Quantitative RT-PCR analysis of indicated transient receptor protein (TRP) channels in (continued)

and outcome. The levels of inflammatory cytokines (interleukin [IL]-1β, tumor necrosis factor [TNF]-α, and IL-6) associate with decreased survival in patients with CKD.[5,6] In addition, we showed a disease stage-dependent upregulation of IL-1α in CKD-derived monocytes and identified IL-1α as key mediator of leukocyte-endothelial adhesion in acute myocardial infarction and CKD with genetic ablation of IL-1 α ameliorating CKD and CVD in the corresponding animal models.[7]

Spatial and temporal regulation of Ca^{2+} signals is essential for initiating but also terminating inflammation, making a dysregulated Ca^{2+} homeostasis a common factor in several autoimmune and inflammatory diseases. In myeloid cells, intracellular Ca^{2+} was shown to regulate nucleotide-binding oligomerization domain (NOD)–like receptor family, pyrin domain–containing 3 inflammasome formation, nitric oxide production, TNF-α and IL-1β release, as well as phagocytosis.[8–10] The main pathways for Ca^{2+} influx in the immune cells include the store-operated Ca^{2+} entry (SOCE); the P2X family of purinergic receptors; and, to a lesser extent, distinct members of the transient receptor protein (TRP) family and other channels.[11,12] The relative contribution of these pathways depends largely on immune cell type and is significantly different between adaptive and innate immune cells.[13] Particularly relevant to CKD is the finding that CKD-derived peripheral mononuclear blood cells showed disturbed Ca^{2+} homeostasis with indications of higher contribution of purinergic signaling.[14] However, the cell type dependence and the pathophysiological consequences of these alterations remained elusive. Furthermore, we and others have shown that Ca^{2+} signals are essential for caspase-1–mediated IL-1β cleavage and activation.[15,16] Moreover, chelating intracellular or extracellular Ca^{2+} results in partial or complete impairment of oxalate acid– or oleic acid–induced IL-1α release, respectively.[7]

Therefore, the aim of this study was to identify molecular players that cause altered Ca^{2+} signatures observed in CKD monocytes and potentially play a role in disease progression, as well as to identify the outcome of altered Ca^{2+} signaling in terms of inflammatory responses and IL-1α production. Herein, we show that purinergic signaling is the main altered pathway in CKD monocytes and that P2X7 plays a significant role in regulation of IL-1α release and thereby to CKD-related inflammatory processes, including cardiac remodeling.

METHODS

Additional materials and methods are described in Supplementary Materials and Methods.

Animal studies

All animal experiments were performed according to the German legislation on protection of animals and the National Institutes of Health *Guide for the Care and Use of Laboratory Animals* (Institute of Laboratory Animal Resources, National Research Council) and reported using the Animal Research: Reporting of In Vivo Experiments (ARRIVE)1 reporting guidelines.[17] All experiments were performed according to the ethical votes 20/2018 and 20/2020 granted approval by the local governmental animal protection committee of Saarland, Germany. Details of the used animal strains are mentioned in the Supplementary Materials and Methods.

Human samples

Patients with stable CKD were recruited at the nephrological outpatient clinic or at the dialysis unit in Saarland University Hospital. CKD severity was evaluated using glomerular filtration rate according to the Kidney Disease: Improving Global Outcomes guidelines.[18,19] Details of the clinical characterization of the patients are listed in Supplementary Table S1. Healthy subjects were recruited from the employees of the Saarland University Hospital with the prerequisite of not having prevalent CVD or CKD, diabetes, or regular medication. All participants signed a written consent, and the study was approved by the local institutional review committee (155/13). Further details to isolation of human monocytes are mentioned in the Supplementary Materials and Methods.

RESULTS

CKD-derived monocytes show altered purinergic Ca^{2+} signatures

To investigate if CKD is associated with alterations of Ca^{2+}-dependent processes, we systematically compared Ca^{2+} profiles of CKD- or healthy control individual–derived monocytes (Figure 1a). First, we measured SOCE, which is mediated by a channel complex formed by a Ca^{2+} selective ion channel (ORAI1-3) and the endoplasmic reticulum–resident Ca^{2+} sensor activator proteins.[20,21] Inducing endoplasmic reticulum store depletion by thapsigargin resulted in a SOCE that was unaltered in CKD compared with the control monocytes (Figure 1b). Similarly, expression of the channel components was comparable in CKD and control individuals (Figure 1c). Next, we analyzed transient receptor potential (TRP) melastatin 2 (TRPM2)–mediated Ca^{2+} influx, which can be activated by cyclic adenosine diphosphate–ribose or hydrogen peroxide (H_2O_2) and is essential for monocyte activation and chemokine production[22] and for IL-1β production in sterile inflammation.[16]

Figure 1 | (continued) control or CKD monocytes. (**f**) Average traces showing changes of F340/F380 over time in response to application of 2 mM adenosine triphosphate (ATP) and corresponding quantification of the AUC measured in control or CKD monocytes. (**g**) Quantitative RT-PCR analysis of indicated P2X ionotropic receptors in cells isolated as in (**a**). Ca^{2+} imaging traces are represented as average traces or bar graphs of average ± SEM obtained from 5 to 10 donors, each 1 to 3 independent experiments the average of each is shown as single dot and total number of cells ranges from 402 to 918 cells. Asterisks indicate significance at $^{*}P < 0.05$ or $^{**}P < 0.01$. ROS, reactive oxygen species; STIM, stromal interaction molecule; TRP, transient receptor potential; TRPC, transient receptor potential canonical; TRPM, transient receptor potential melastatin; TRPV, transient receptor potential vanilloid.

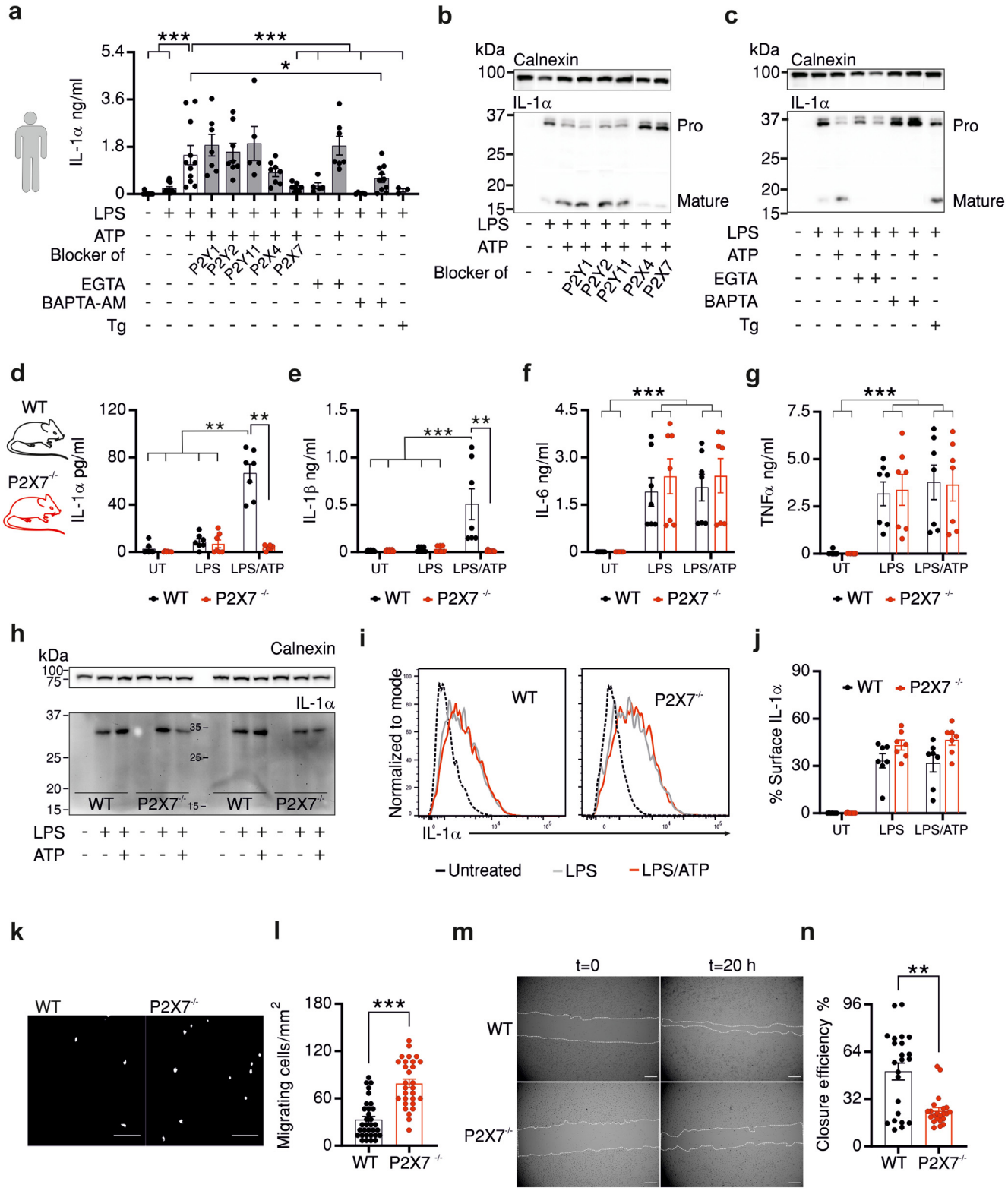

Figure 2| P2X7-mediated Ca^{2+} influx is essential for adenosine triphosphate (ATP)–induced release of interleukin (IL)-1α with P2X7$^{-/-}$ bone marrow–derived macrophages (BMDMs) showing abrogated release but increased surface presentation of IL-1α. (**a**) Enzyme-linked immunosorbent assay (ELISA) measurements showing IL-1α released by human $CD14^{+}$ monocytes (dots represent independent donors) in response to 100 ng/ml lipopolysaccharide (LPS) overnight priming and 2 mM ATP 30-minute application without or with pretreatment with blockers of the indicated purinergic receptors, 2 mM ethyleneglycol-bis-(β-aminoethylether)-*N,N,N′,N′*-tetraacetic acid (EGTA) or 50 μM BAPTA-AM (1,2-bis(*o*-aminophenoxy)ethane-*N,N,N′,N′*-tetraacetic acid acetoxymethyl ester), as indicated. (**b,c**) Representative of 3 Western blots showing analysis of intracellular IL-1α from monocytes treated as in (**a**). (**d–g**) ELISA measurement showing IL-1α, IL-1β, IL-6, or tumor necrosis factor (TNF)-α release by murine BMDMs derived from wild-type (WT; black) or P2X7$^{-/-}$ (red) (continued)

H_2O_2-induced Ca^{2+} influx was comparable in CKD and control monocytes (Figure 1d). Furthermore, expression levels of TRPM2 and other members of the TRP channel family (TRP vanilloid 1 [TRPV1], TRP canonical 1 [TRPC1], TRPC3, TRPC6, and TRPM7) potentially contributing to Ca^{2+} signals in monocytes[23,24] were not altered in CKD monocytes (Figure 1e). Finally, we investigated purinergic signaling, previously shown essential for inflammasome activation in monocytes.[10] Adenosine triphosphate (ATP) application induced a biphasic response in human monocytes where the first component mostly represents ATP-induced release of Ca^{2+} from intracellular stores by activation of the metabotropic Gq-coupled P2Y receptors and the second component represents Ca^{2+} influx through the ionotropic P2X channels. ATP induced a significantly stronger Ca^{2+} influx in CKD compared with control monocytes mainly during the second phase, indicated by the significant increase of the area under the curve (Figure 1f). Expression analysis showed increased expression of the ionotropic P2X4 and P2X7 receptors (gene names *P2RX4* and *P2RX7*, respectively; Figure 1g), whereas expression of the metabotropic receptors (P2Y) was not overtly altered (Supplementary Figure S1A), suggesting that P2X7 and P2X4 regulate Ca^{2+}-dependent immune functions of monocytes in CKD.

P2X7-mediated Ca^{2+} influx is essential for ATP-induced release of IL-1α with $P2X7^{-/-}$ bone marrow–derived macrophages, showing abrogated release but increased surface presentation of IL-1α

To directly address the purinergic dependency of IL-1α secretion, we preincubated primed monocytes with blockers of selected members of P2Y and P2X receptors and then measured IL-1α release. Inhibiting P2Y receptors did not alter ATP-induced IL-1α release, inhibiting P2X4 resulted in a nonsignificant reduction, while inhibiting P2X7 abolished ATP-induced IL-1α release (Figure 2a). We observed comparable effects on IL-1β release, although less prominent (Supplementary Figure S1B). Next, we investigated the effect of Ca^{2+} chelation on IL-1α release. In contrast to chelating extracellular Ca^{2+} with ethyleneglycol-bis-(β-aminoethylether)-*N*,*N*,*N*′,*N*′-tetraacetic acid (EGTA), chelating intracellular Ca^{2+} using 1,2-bis(*o*-aminophenoxy)ethane-*N*,*N*,*N*′,*N*′-tetraacetic acid acetoxymethyl ester (BAPTA-AM) reduced IL-1α release. On the other hand, increasing $[Ca^{2+}]_i$ per se by releasing intracellular stores with thapsigargin in lipopolysaccharide (LPS) primed cells was not sufficient to trigger IL-1α release in absence of ATP treatment (Figure 2a).

Corresponding Western blot analysis of monocyte lysates showed that resting cells do not express detectable levels of IL-1α but that LPS treatment induced upregulation of IL-1α with the proform being more prominent (Figure 2b). ATP reduces the total intracellular content of IL-1α with concomitant accumulation in the supernatant, as measured by enzyme-linked immunosorbent assay (Figure 2a). Notably, treatment of LPS-primed cells with ATP induces cleavage of IL-1α, resulting in detectable levels of the mature form in cell lysates, which was reduced by blocking either P2X4 or P2X7 (Figure 2b). Furthermore, Western blot analysis showed that processing of the proform into mature IL-1α was inhibited by chelating both intracellular and extracellular Ca^{2+} but enhanced with thapsigargin treatment (Figure 2c).

Together, these results indicate that although both P2X4 and P2X7 are involved in processing of IL-1α, P2X7 signaling has a more prominent role in ATP-induced IL-1α release. In addition, these results implicate that not only the Ca^{2+} levels per se but also ATP-induced intracellular signaling are necessary for IL-1α release. To confirm the role of P2X7 in regulating IL-1α release, we measured IL-1α release from bone marrow–derived macrophages (BMDMs) from P2X7 knockout mice ($P2X7^{-/-}$). Results (Figure 2d and e) depict that genetic ablation of *P2XR7* ($P2X7^{-/-}$) completely abolished ATP-induced release of both IL-1α and IL-1β, in line with results obtained from human monocytes (Figure 2a and Supplementary Figure S1A), whereas the release of IL-6 and TNF-α were comparable in $P2X7^{-/-}$ and wild-type (WT) derived cells (Figure 2f and g). In contrast to IL-1β,[25] the role of P2X7 in biogenesis of IL-1α is not fully characterized. To delineate whether the inability of $P2X7^{-/-}$ BMDMs to produce IL-1α is due to altered expression or impaired secretion mechanisms, we analyzed intracellular IL-1α expression and observed that $P2X7^{-/-}$ cells primed with LPS showed comparable upregulation of IL-1α to WT cells, suggesting that P2X7 is involved in regulation of release mechanisms but not of LPS-induced transcription of IL-1α (Figure 2h). Because we have previously shown that membrane-bound IL-1α is essential for adhesion of immune cells,[7] we explored the membrane-bound fraction of IL-1α in $P2X7^{-/-}$ cells. Flow cytometry experiments showed that $P2X7^{-/-}$ BMDMs exhibit an accumulation of surface IL-1α compared with WT cells (Figure 2i and j). Notably, we observed similar phenotypes in $P2X7^{-/-}$ compared with WT circulating monocytes (Supplementary Figure S2A–F). To examine the influence of the accumulating membrane-bound IL-1α, we assessed the migration potential of

Figure 2 | (continued) mice, starved overnight (untreated cell [UT]) and primed with 100 ng/ml LPS for 4 hours (LPS) before application of 2mM ATP (LPS/ATP). (**h**) Representative of 3 Western blots showing expression of IL-1α in cells measured in (**d–g**). (**i**) Representative flow cytometry analysis and (**j**) quantification of fraction of cells showing IL-1α surface expression in cells measured in (**d–g**). (**a–j**) Dots depict individual human donors or mice used in each experiment. (**k**) Representative images (bar = 100 μm) and (**l**) quantification of migrating BMDMs isolated from WT or $P2X7^{-/-}$ and seeded in a transwell migration assay. At 16 hours later, cells on the basolateral side were stained with Hoechst 33342 and counted. (**m**) Representative images (bar = 1 mm) acquired after making a scratch in a monolayer of WT or $P2X7^{-/-}$ BMDMs or 20 hours later. (**n**) Efficiency of scratch closure of measurements in (**m**). (**l,n**) Dots represent 3 to 5 replicate fields analyzed from n = 6 mice in each condition, and asterisks indicate significance at $^*P < 0.05$, $^{**}P < 0.01$, and $^{***}P < 0.001$. Tg, thapsigargin. Antibodies used are listed in Supplementary Table S4. To optimize viewing of this image, please see the online version of this article at www.kidney-international.org.

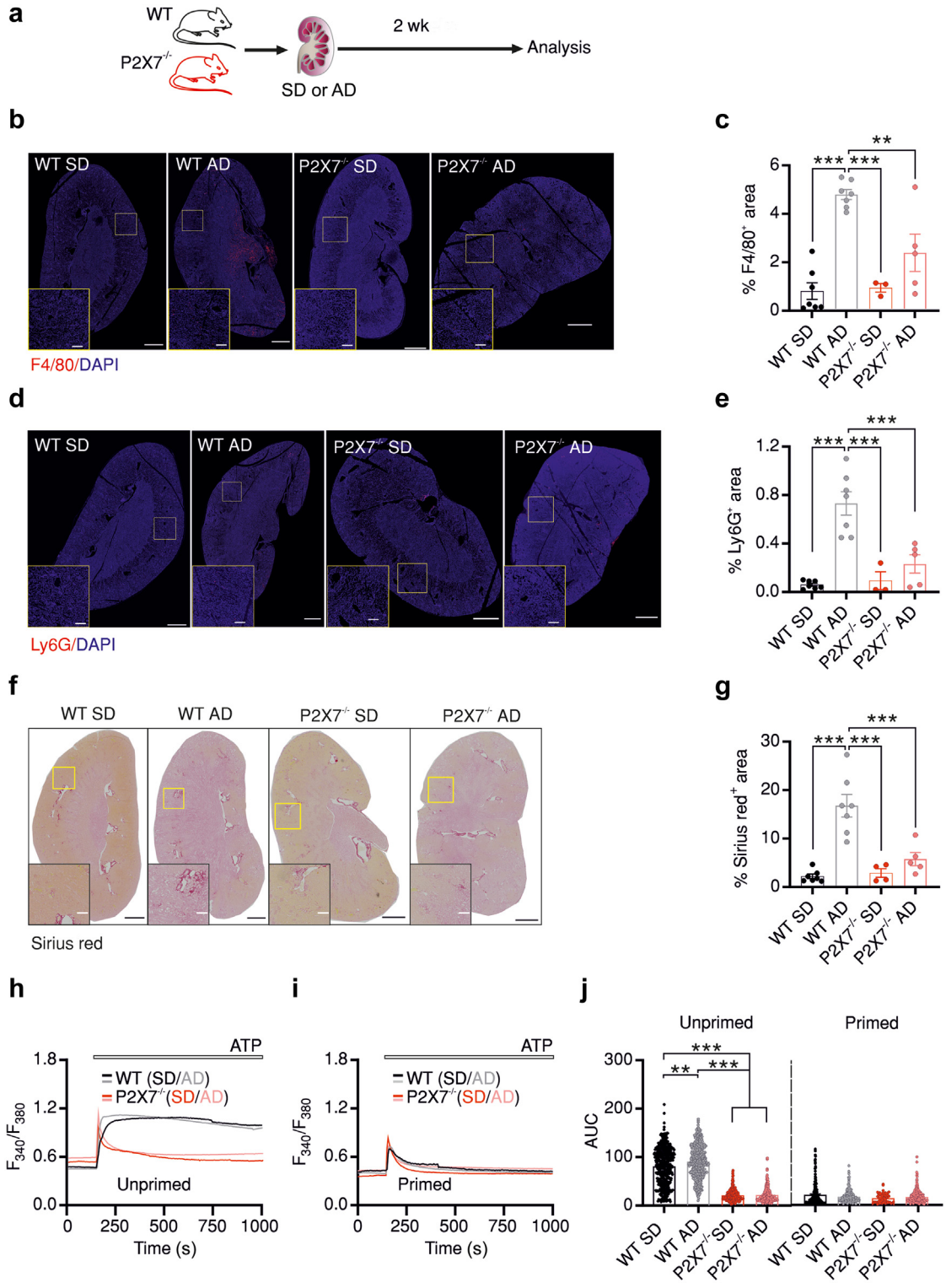

Figure 3 | Genetic ablation of P2X7 reduces Ca^{2+} signals in macrophages and abrogates kidney infiltration during chronic kidney injury. (**a**) Schematic representation of the kidney injury model: wild-type (WT; black) or $P2X7^{-/-}$ (red) mice were subjected to standard diet (SD) or 0.2% adenine diet (AD) for 2 weeks before analysis. Representative images of kidney sections from mice fed with SD or AD and corresponding quantification of infiltration by (**b,c**) $F4/80^+$ macrophages, (**d,e**) $Ly6G^+$ neutrophils, and (**f,g**) Sirius red^+ fibrotic areas. Bar = 500 μm in overview images and 150 μm in the insets. (**h**) Average traces showing measurement of adenosine triphosphate (ATP)–induced Ca^{2+} influx in bone marrow–derived macrophages isolated from WT (black and gray) or $P2X7^{-/-}$ mice (red and pink) subjected to indicated diet in (**h**) unprimed state (unprimed) or (**i**) following priming with lipopolysaccharide (primed). (**j**) Bar graphs showing average area under the ATP response curve (AUC) of measurements in (**h,i**). Ca^{2+} imaging traces depict average trace of a representative experiment, and corresponding bar graphs show single cells (229–503 cells) derived from 4 to 7 mice per group, as indicated by the number of (continued)

BMDMs. Concomitant to surface IL-1α accumulation, P2X7$^{-/-}$ BMDMs showed a significant increase in migrating cell numbers in a transwell migration assay (Figure 2k and l). However, P2X7$^{-/-}$ BMDMs demonstrated a significantly reduced efficiency of wound closure when challenged in a wound healing assay (Figure 2m and n). Together, these findings suggest that genetic ablation of P2X7 results in multiple alterations in immune cells that might affect the outcome of the immune response.

Genetic ablation of P2X7 reduces Ca^{2+} signals in macrophages and abrogates kidney infiltration during chronic kidney injury

Next, we investigated the role of P2X7 in inflammation-mediated kidney injury, which has been addressed previously, but the outcome was controversial depending on the applied experimental model.[26,27] A 2-week 0.2% adenine diet (AD; Figure 3a) resulted in comparable elevations of creatinine and urea levels in both WT and P2X7$^{-/-}$ mice (Supplementary Figure S2G and H). However, P2X7$^{-/-}$ mice exhibited a decrease in AD-induced infiltrating F4/80^{+} macrophages and Ly6G^{+} neutrophils, as well as a reduction in Sirius red^{+} fibrotic area (Figure 3b–g), indicating the involvement of P2X7 in the development of kidney injury.

Investigation of concomitant alterations in Ca^{2+} homeostasis of corresponding BMDMs showed that compared with the standard diet, subjecting WT mice to high AD resulted in reduced maximal (Peak; Supplementary Figure S2I and J) but not sustained (Plateau; Supplementary Figure S2I and K) thapsigargin-induced Ca^{2+} entry. These alterations were not overtly affected by deletion of P2X7. In contrast, AD resulted in an enhancement of ATP-induced Ca^{2+} influx in unprimed WT but not P2X7$^{-/-}$ derived BMDMs (Figure 3h and j). Deletion of P2X7 resulted in strong reduction of ATP-induced Ca^{2+} influx in unprimed knockout BMDMs (Figure 3h and j), supporting that P2X7 is the main mediator of ATP-induced Ca^{2+} influx in BMDMs. A similar reduction of ATP-induced Ca^{2+} influx was observed in circulating monocytes (Supplementary Figure S3A and B). Noteworthy, priming WT BMDMs with LPS resulted in a dramatic decrease in ATP-induced Ca^{2+} entry independent of the administered diet and without additional impact of P2X7 deletion (Figure 3i and j). To test whether this reduction is specific to murine cells, we also measured ATP-induced Ca^{2+} influx in LPS-primed human monocytes. Results (Supplementary Figure 3C and D) show that similar to the murine cells, but to a weaker extent, priming human monocytes with LPS led to significant reduction of ATP-induced Ca^{2+} influx. Expression analysis demonstrated that although in both human and murine cells, P2X7 expression is not overtly altered, LPS priming resulted in significant upregulation of P2X4 (Supplementary Figure 3E and F), in agreement with a previous study[28] and potentially explaining the LPS-induced alteration of Ca^{2+} influx.

P2X7 is dispensable for accumulation of IL-1α in acutely injured cardiac tissue

IL-1α$^{-/-}$ immune cells are less recruited to injured cardiac tissues,[7] but the P2X7 dependency of this observation is not known. Subjecting WT mice to permanent left anterior descending artery (LAD) ligation to simulate myocardial infarction (MI; Figure 4a) resulted in Ly6G^{+} neutrophil infiltration and an increase in IL-1α^{+} cells in cardiac tissues compared with sham operated mice (Figure 4b–e). Genetic ablation of P2X7 did not alter LAD-induced neutrophil infiltration (Figure 4b and c) or IL-1α accumulation in P2X7$^{-/-}$ hearts (Figure 4d and e), indicating that P2X7 deletion is not sufficient to abolish cardiac injury-induced immune cell infiltration or upregulation of IL-1α.

Parallel investigation of Ca^{2+} profiles in corresponding BMDMs demonstrated that although WT cells showed unaltered SOCE, LAD ligation increased SOCE in P2X7$^{-/-}$ mice compared with WT cells but not BMDMs derived from P2X7$^{-/-}$ sham operated mice (Supplementary Figure S3F–H). Similar to observations (Figure 3), ATP-induced Ca^{2+} entry was significantly reduced in P2X7$^{-/-}$ compared with WT unprimed BMDMs (Figure 4f and h). Again, priming with LPS strongly decreased ATP-induced Ca^{2+} entry in both sham and MI operated mice (Figure 4g and h). Together, these results indicate that genetic ablation of P2X7 affects Ca^{2+} homeostasis of immune cells by directly mediating ATP-induced Ca^{2+} influx and indirectly by modulating SOCE, with implications for their potential to induce inflammation also in later stages postinfarction.

Because CKD is a significant risk factor for developing CVD,[29] we investigated the effect of P2X7 deletion in a combined CKD/MI model (Figure 5a). Image analyses showed that cardiac infiltration by Ly6G^{+} cells was nonsignificantly ameliorated (Figure 5b and c), and the fraction of IL-1α^{+} cells was not altered by deletion of P2X7 (Figure 5d and e). SOCE was not overtly altered in WT or P2X7$^{-/-}$ BMDMs in response to the combined injury (Supplementary Figure S3I–K). On the other hand, combined injury increased ATP-induced Ca^{2+} influx in primed but not unprimed WT BMDMs while P2X7$^{-/-}$ BMDMs were resistant (Figure 5f–h).

To gain more insight into the immunomodulatory role of P2X7, we investigated the immune profile of corresponding BMDMs. Interestingly, the proinflammatory cytokines IL-1α (Figure 5i) and IL-1β (Supplementary Figure S4A) released by WT-derived BMDMs were not altered by combining kidney and cardiac injury procedures. Importantly, similar to observations (Figure 2d–j), secretion of both cytokines was

Figure 3 | (continued) dots in the corresponding image analysis bar graphs of the same group. Asterisks indicate significance at $^{*}P < 0.05$, $^{**}P < 0.01$, and $^{***}P < 0.001$. DAPI, 4′,6-diamidino-2-phenylindole. Antibodies used are listed in Supplementary Table S4. To optimize viewing of this image, please see the online version of this article at www.kidney-international.org.

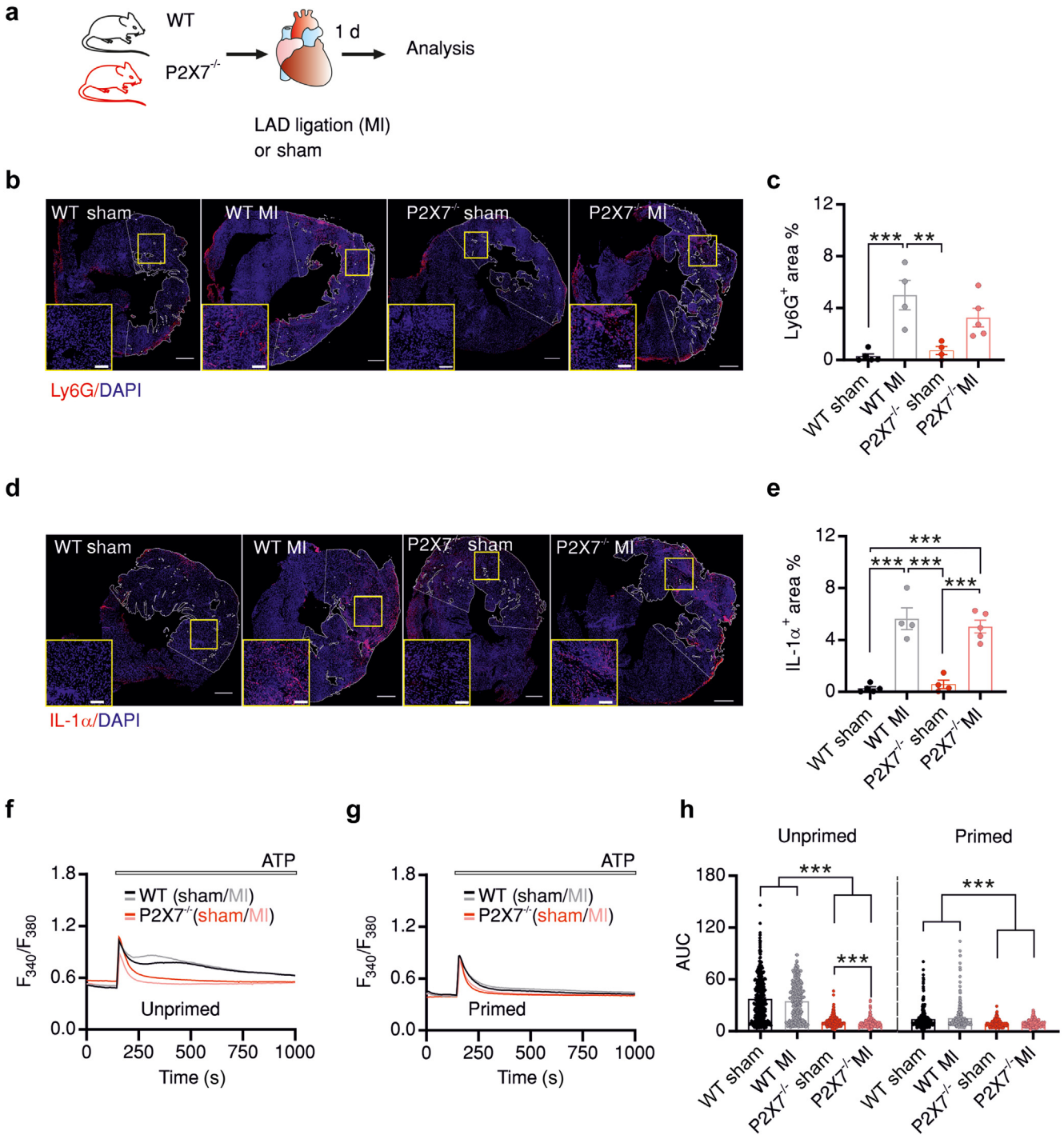

Figure 4 | Genetic ablation of P2X7 does not alter infiltration of immune cells or upregulation of interleukin (IL)-1α in injured cardiac tissues. (**a**) Schematic representation of myocardial infarction (MI) model: wild-type (WT); black) or P2X7$^{-/-}$ (red) mice were subjected to left anterior descending artery (LAD) ligation (MI) or sham operation 24 hours before analysis. Representative images of heart sections from mice treated as in (**a**) and quantification of fraction of infiltrating by (**b,c**) Ly6G^{+} neutrophils or (**d,e**) cells expressing IL-1α. Bar represents 500 μm in overview images and 150 μm in the insets. (**f,g**) Average traces showing measurements of adenosine triphosphate (ATP)–induced Ca^{2+} influx in bone marrow–derived macrophages isolated from WT (black and gray) or P2X7$^{-/-}$ mice (red and pink) treated as in (**a**). Measurements were done in (**f**) resting cells (unprimed) or (**g**) following priming with 100 ng/ml lipopolysaccharide (primed). (**h**) Bar graphs showing average area under the ATP response curve (AUC) of cells measured in (**f,g**). Ca^{2+} imaging traces depict average trace of a representative experiment, and corresponding bar graphs show single cells (309–454 cells) derived from 4 to 5 mice per group, as indicated by the number of dots in the corresponding image analysis bar graphs of the same group. Asterisks indicate significance at $^{*}P < 0.05$, $^{**}P < 0.01$, and $^{***}P < 0.001$. DAPI, 4′,6-diamidino-2-phenylindole. Antibodies used are listed in Supplementary Table S4. To optimize viewing of this image, please see the online version of this article at www.kidney-international.org.

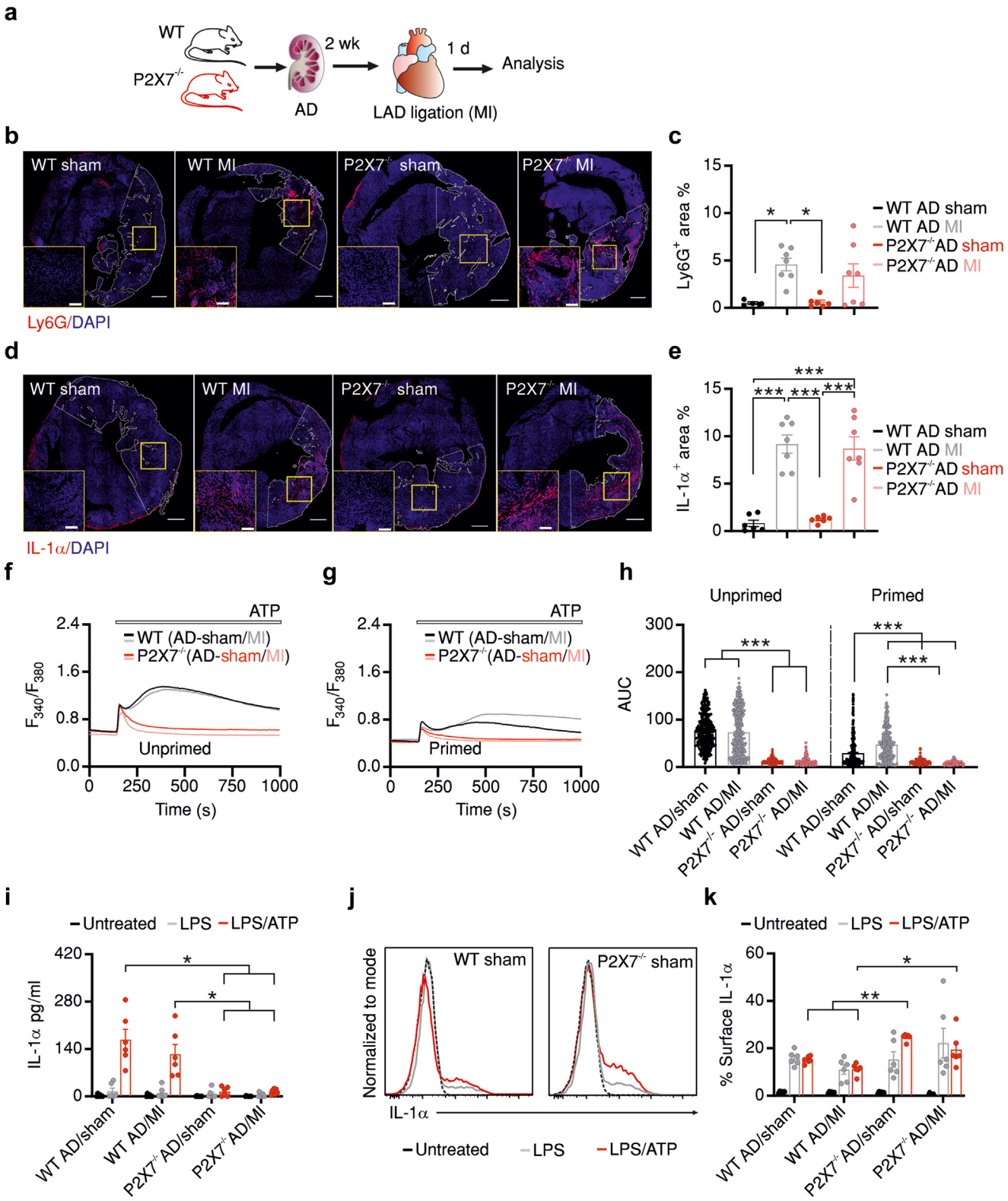

Figure 5 | Genetic ablation of P2X7 abrogates secretion but facilitates surface accumulation of interleukin (IL)-1α in bone marrow–derived macrophages (BMDMs) associated with cardiac injury. (**a**) Schematic representation of combined kidney and cardiac injury model: wild-type (WT; black) or P2X7$^{-/-}$ (red) mice were fed with 0.2% adenine diet (AD) for 2 weeks and then subjected to left anterior descending artery (LAD) ligation (myocardial infarction [MI]) or sham operation 24 hours before analysis. Representative images of heart sections from mice treated as in (**a**) and quantification of fraction of infiltrating by (**b,c**) Ly6G^{+} neutrophils or (**d,e**) cells expressing IL-1α. (**f,g**) Average traces showing measurements of adenosine triphosphate (ATP)–induced Ca^{2+} influx in BMDMs isolated from WT (black and gray) or P2X7$^{-/-}$ mice (red and pink) treated as in (**a**). Measurements were done in (**f**) resting cells (unprimed) or (**g**) following priming with 100 ng/ml (continued)

completely abrogated in P2X7$^{-/-}$ BMDMs (Figure 5i and Supplementary Figure S4A), whereas there was a higher fraction of IL-1α^{+} cells in P2X7$^{-/-}$ compared with WT cells in both sham and LAD-operated mice (Figure 5j and k) while intracellular levels were not altered (Supplementary Figure S4B).

These findings indicate that also in the context of combined CKD and MI, P2X7 is essential in regulating Ca^{2+} signaling in both unprimed and primed macrophages as well as regulating processing and release of IL-1α with abrogated secretion but increased surface presentation of IL-1α on P2X7 deletion.

P2X7 plays a pivotal role in organ-immune cell interaction during inflammation and exposure to injury

To distinguish between the impact of P2X7 deletion in immune cells versus nonimmune organs, we created 2 bone marrow chimeric mouse lines to delete P2X7 on either immune cells (Ch1) or other organs (Ch2) of chimeric lines that were sham or LAD operated (Figure 6a). We confirmed the efficiency of chimerism by amplifying a P2X7-specific genomic region, as in a previous study,[30] from genomic DNA isolated from chimeric BMDMs (Supplementary Figure S4C and D). Histologic analysis showed an LAD-induced mild increase in the fraction of Ly6G^{+}, which was equal for cardiac tissues of both chimeras (Figure 6b and c). Noteworthy, this increase was much less prominent than what we observed in the single cardiac and combined cardiorenal injury models (Figures 4c and 5c), although while drawing this conclusion one has to consider that these procedures and corresponding analyses were not done in parallel. Interestingly, the fraction of IL-1α^{+} cells in the infarction area was significantly lower in Ch1 lacking P2X7 on the immune cells (Figure 6d and e), indicating a role of P2X7 in regulating cardiac IL-1α in response to infarction.

BMDMs derived from Ch1 (harboring P2X7$^{-/-}$ BMDMs) showed the expected reduction of ATP-induced Ca^{2+} influx (Figure 6f–h; black and gray), whereas Ch2 showed a biphasic Ca^{2+} influx (Figure 6f–h; red and pink) characteristic of WT BMDMs (see Figures 3h and 4f). Interestingly, inducing cardiac injury in Ch2 resulted in a significant reduction of ATP-induced Ca^{2+} influx in unprimed BMDMs (Figure 6f and h) in contrast to the same intervention in WT mice (Figures 4 and 5). This finding indicates that the lack of P2X7 in nonimmune mouse tissues in Ch2 has a significant influence on the Ca^{2+} homeostasis of immune cells, especially under disease conditions.

Next, we investigated the immune profile of both chimeras. As predicted for cells lacking P2X7, ATP-induced IL-1α and IL-1β release by Ch1 was abolished. In contrast, WT BMDMs of Ch2 mice showed compromised release of IL-1α or IL-1β in response to ATP (Figure 6i and Supplementary Figure S4E) compared with nonchimeric mice (Figure 2d and e). Furthermore, P2X7$^{-/-}$ BMDMs in Ch1 showed a slight accumulation of membrane-bound IL-1α compared with Ch2, but alterations were not significant (Figure 6j and k). Remarkably, the attenuation of cytokine release by Ch2 was specific to IL-1α and IL-1β because released IL-6 and TNF-α (Supplementary Figure S4F and G) by both chimeras were comparable to nonchimeric mice (Figure 2f and g).

In the cardiac injury models described so far, we evaluated inflammatory processes during the acute phase following cardiac injury. To investigate whether genetic ablation of P2X7 alters the severity of chronic injury, we evaluated cardiac function using noninvasive echocardiography 2 weeks after the surgical procedures (Figure 7a). This time period was sufficient for cardiac tissues to recover from acute inflammation, as indicated by exhibiting a control fraction of infiltrating immune cells and a reversal of IL-1α upregulation (Supplementary Figure S4H and I, images not shown, compared with Figures 4 and 5). Findings (Figure 7b–f and Supplementary Table S5) illustrate that P2X7$^{-/-}$ and Ch1 (harboring P2X7$^{-/-}$ immune cells) mice were protected against LAD-induced heart structural or functional alterations. In strong contrast, parasternal long and short axis images at end diastolic and systolic positions of Ch2 hearts (harboring WT immune cells) show LAD ligation induced profound dilatation of the left ventricle (LV) to extents comparable to the remodeling observed in injured WT mice (Figure 7b and c). Furthermore, recordings of LV systolic function demonstrated that both WT and Ch2 LAD-operated mice exhibited marked apical and anterior wall hypokinesia to akinesia with preserved pump function only in basal parts of the LV compared with corresponding sham operated mice. These changes reflect a profoundly compromised cardiac function, as indicated by the significantly reduced ejection fraction (Figure 7d and e) and significantly elevated LV end volumes of Ch2 (Figure 7f).

These findings strongly point to an essential role of immune cell–P2X7 in modulating inflammation-dependent cardiac remodeling following MI.

Figure 5 | (continued) lipopolysaccharide (LPS; primed). (**h**) Bar graphs showing average area under the ATP response curve (AUC) of cells measured in (**f,g**). (**i**) Enzyme-linked immunosorbent assay measurement showing IL-1α release by BMDMs derived from WT or P2X7$^{-/-}$ mice, starved overnight (untreated; black) and primed with 100 ng/ml LPS for 4 hours (LPS; gray) before application of 2 mM ATP (LPS/ATP; red). (**j**) Representative flow cytometry analysis and (**k**) quantification of fraction of cells showing surface IL-1α expression in cells measured in (**i**). Ca^{2+} imaging traces depict average trace of a representative experiment, and corresponding bar graphs show single cells (293–492 cells) derived from 6 to 7 mice per group, as indicated by the number of dots in the corresponding image analysis bar graphs of the same group. Asterisks indicate significance at $^{*}P < 0.05$, $^{**}P < 0.01$, and $^{***}P < 0.001$. DAPI, 4′,6-diamidino-2-phenylindole. Antibodies used are listed in Supplementary Table S4. To optimize viewing of this image, please see the online version of this article at www.kidney-international.org.

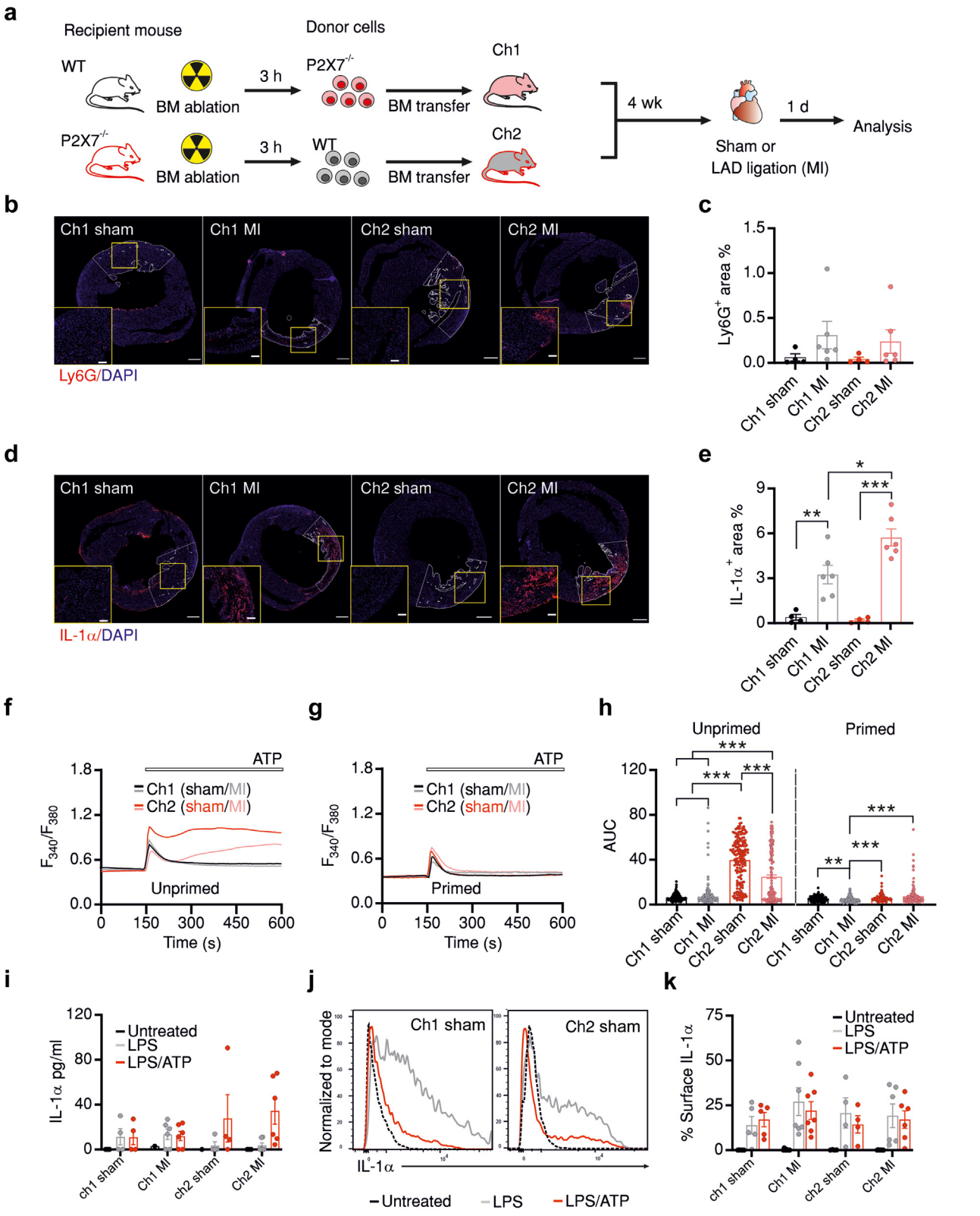

Figure 6 | P2X7 deletion on immune or heart cells ameliorates acute inflammation after cardiac injury. (**a**) Schematic representation of the experimental design of generating chimeric mice: chimera 1 (Ch1) was generated using wild-type (WT) mice as recipient and P2X7$^{-/-}$ mice as bone marrow (BM) donor, and chimera 2 (Ch2) was generated vice versa. Procedure details are mentioned in Methods section. Chimeric lines were subjected to left anterior descending artery (LAD) ligation (myocardial infarction [MI]) or sham operation 24 hours before analysis. Representative images of heart sections from mice treated as in (**a**) and quantification of fraction of infiltrating by (**b,c**) Ly6G^{+} neutrophils or (**d,e**) cells expressing IL-1α. Bar represents 500 μm in overview images and 150 μm in the insets. (**f,g**) Average traces showing (continued)

Mitochondrial reactive oxygen species are necessary for regulation of IL-1α secretion by P2X7

In the next section, we sought to decipher the molecular mechanisms underlying the immunomodulatory role of P2X7. In astrocytes, microglia, and monocytes, P2X7-dependent reactive oxygen species (ROS) production was shown necessary for IL-6 and IL-1β release.[31–33] However, if IL-1α release is dependent on P2X7-induced ROS is unknown. Therefore, we transfected a human monocyte cell line (U937) with mitochondrial- or cytosolic-targeted H_2O_2 sensor (HyPer7) and measured alterations in $[H_2O_2]$ in response to ATP in control or cells pretreated with the P2X7 inhibitor (A804598). Illuminating the cells with the sensor-specific wave lengths resulted in a steady increase of fluorescent ratio (see individual experiments in Supplementary Figure S5). To unambiguously correlate the fluorescence increase to ATP-mediated P2X7 activation, control experiments were performed by applying ATP-free buffer and by confirming sensor reactivity with a terminal application of H_2O_2. Ratiometric measurements showed that ATP results induce a significant and P2X7-dependent increase in mitochondrial but not cytosolic H_2O_2 (Figure 8a–c). Pretreating the cells with a cell membrane-permeable Ca^{2+} chelator (BAPTA-AM) abolished mitochondrial ROS production (Supplementary Figure S5G and H), indicating the Ca^{2+} dependency of ATP-induced mitochondrial ROS.

To further investigate ROS-dependent IL-1α release, we used 2 mouse lines: a knockout of the main source for cytosolic ROS in immune cells, reduced nicotinamide adenine dinucleotide phosphate–oxidase 2 ($NOX2^{-/-}$)[34]; and an overexpression line for mitochondrial catalase, which buffers mitochondrial ROS.[35] Compared with the corresponding WT (BL6/N or BL6/J), inhibition of mitochondrial ROS but not deletion of NOX2 resulted in a significant reduction of IL-1α but not IL-1β (Figure 8d and e). Furthermore, pretreating the cells derived from all examined mouse lines with P2X7 blocker resulted in reduction of the released IL-1α and IL-1β except for the mitochondrial catalase, in which a reduction of IL-1β but not IL-1α was observed, indicating a stronger dependency of IL-1α than IL-1β on P2X7-induced ROS (Figure 8d and e). Concomitantly, flow cytometry showed that reducing mitochondrial but not NOX2-dependent ROS induced a trend of increased surface IL-1α on mitochondrial catalase–derived BMDMs (Figure 8f and g). Finally, we explored whether P2X7 deletion alters the homeostasis of ROS-related proteins. Indeed, compared with WT, P2X7 deletion is accompanied by significant downregulation of the cytosolic ROS scavenger catalase[36] and to a lesser nonsignificant extent peroxiredoxin-2 and the mitochondrial peroxiredoxin-3, whereas superoxide dismutase-2 was not altered (Figure 8h and i).[37] These findings suggest that the protective effect of deleting P2X7 might be partly due to adaptive alterations in ROS levels.

Collectively, our findings implicate that P2X7 plays a pivotal role in regulation of IL-1α contribution to inflammatory processes in kidney and cardiac diseases, and this regulation is dependent on mitochondrial ROS production.

DISCUSSION

The current work identified purinergic signaling as an essential pathway for regulation of IL-1α release. We show that P2X7 is upregulated in CKD monocytes and is the major pathway for ATP-induced Ca^{2+} influx in human monocytes and murine macrophages. The importance of P2X7-mediated regulation of proinflammatory cytokine secretion is highlighted in the context of CKD/MI in the respective animal models. Mechanistically, we identify mitochondrial ROS as an important second messenger linking ATP signaling through P2X7 to IL-1α release. Importantly, chimeric mouse experiments strongly indicate that P2X7 is crucial in monocyte-driven inflammatory processes during the development of kidney insufficiency and persistent cardiac injury.

Purinergic receptors represent a signaling hub that is evidently coupled to Ca^{2+} and ROS signaling and to the metabolic state of cells with implications in tumors and inflammatory diseases.[38–40] Kidney cells are able to release signaling nucleotides (ATP and adenosine diphosphate) and are equipped with purinergic signaling machinery.[39] Functional P2X7 is associated with glomerular injury in models of acute glomerulonephritis[27] and ischemia-reperfusion acute kidney injury.[41] These findings suggest purinergic signaling as a therapeutic target for inflammatory diseases, including CKD and CVD. Although CKD clinical studies using P2X7 blockers have so far been either aborted or did not result in the anticipated outcome,[39] clinical and translational studies support therapeutic potential of P2X7 antagonists in other inflammatory diseases, such as rheumatoid arthritis and obstructive pulmonary diseases.[42,43]

Figure 6 | (continued) measurements of adenosine triphosphate (ATP)–induced Ca^{2+} influx in BM-derived macrophages (BMDMs) isolated from Ch1 (black and gray) or Ch2 mice (red and pink) treated as in (**a**). Measurements were done in (**f**) resting cells (unprimed) or (**g**) following priming with 100 ng/ml lipopolysaccharide (LPS; primed). (**h**) Bar graphs showing average area under the ATP response curve (AUC) of cells measured in (**f,g**). Ca^{2+} imaging traces depict average trace of a representative experiment (50–150 cells), and bar graphs represent average ± SEM obtained from 5 to 6 mice per group. (**i**) Enzyme-linked immunosorbent assay measurement showing interleukin (IL)-1α release by BMDMs derived from Ch1 or Ch2 mice, starved overnight (untreated; black) and primed with 100 ng/ml LPS for 4 hours (LPS; gray) before application of 2 mM ATP (LPS/ATP; red). (**j**) Representative flow cytometry analysis and (**k**) quantification of fraction of cells showing surface IL-1α expression in cells measured in (**i**). Ca^{2+} imaging traces depict average trace of a representative experiment, and corresponding bar graphs show single cells (100–373 cells) derived from 4 to 6 mice per group, as indicated by the number of dots in the corresponding image analysis bar graphs of the same group. Asterisks indicate significance at $^*P < 0.05$, $^{**}P < 0.01$, and $^{***}P < 0.001$. DAPI, 4′,6-diamidino-2-phenylindole. Antibodies used are listed in Supplementary Table S4. To optimize viewing of this image, please see the online version of this article at www.kidney-international.org.

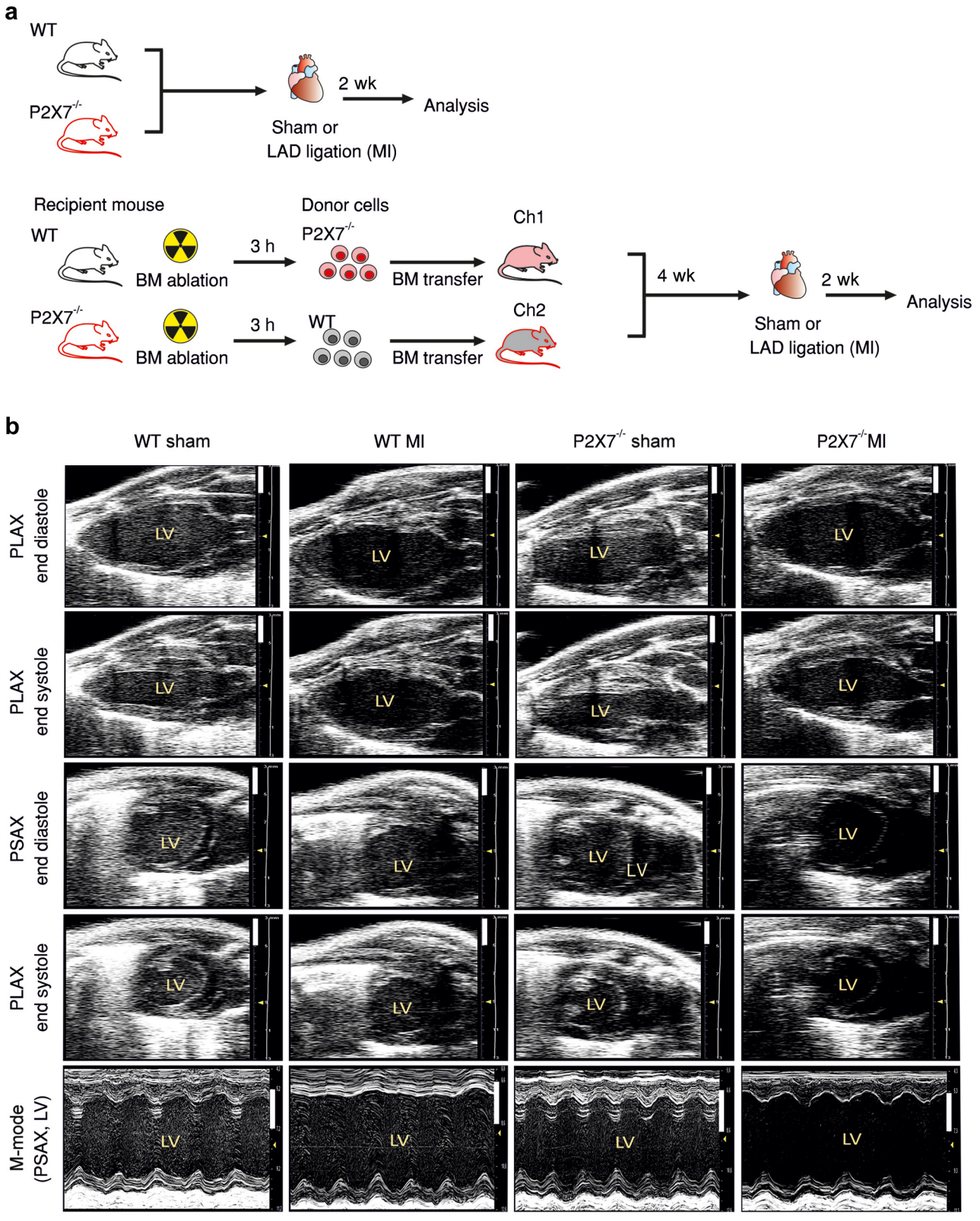

Figure 7 | P2X7 deletion on immune but not on heart cells ameliorates cardiac remodeling after cardiac injury. (**a**) Schematic representation of the experimental design: nonchimeric wild-type (WT), P2X7$^{-/-}$, as well as chimeric lines generated as in Figure 6 were subjected to left anterior descending artery (LAD) ligation (myocardial infarction [MI]) or sham operation 2 weeks before echocardiography analysis was performed. Representative images of measurements done in (**a**) from (**b**) nonchimeric and from (**c**) chimeric mice acquired in parasternal long (PLAX) and short (PSAX S) axis at end diastolic and systolic frames or along PLAX during movement (M-mode). Bar = 2 mm. (Continued)

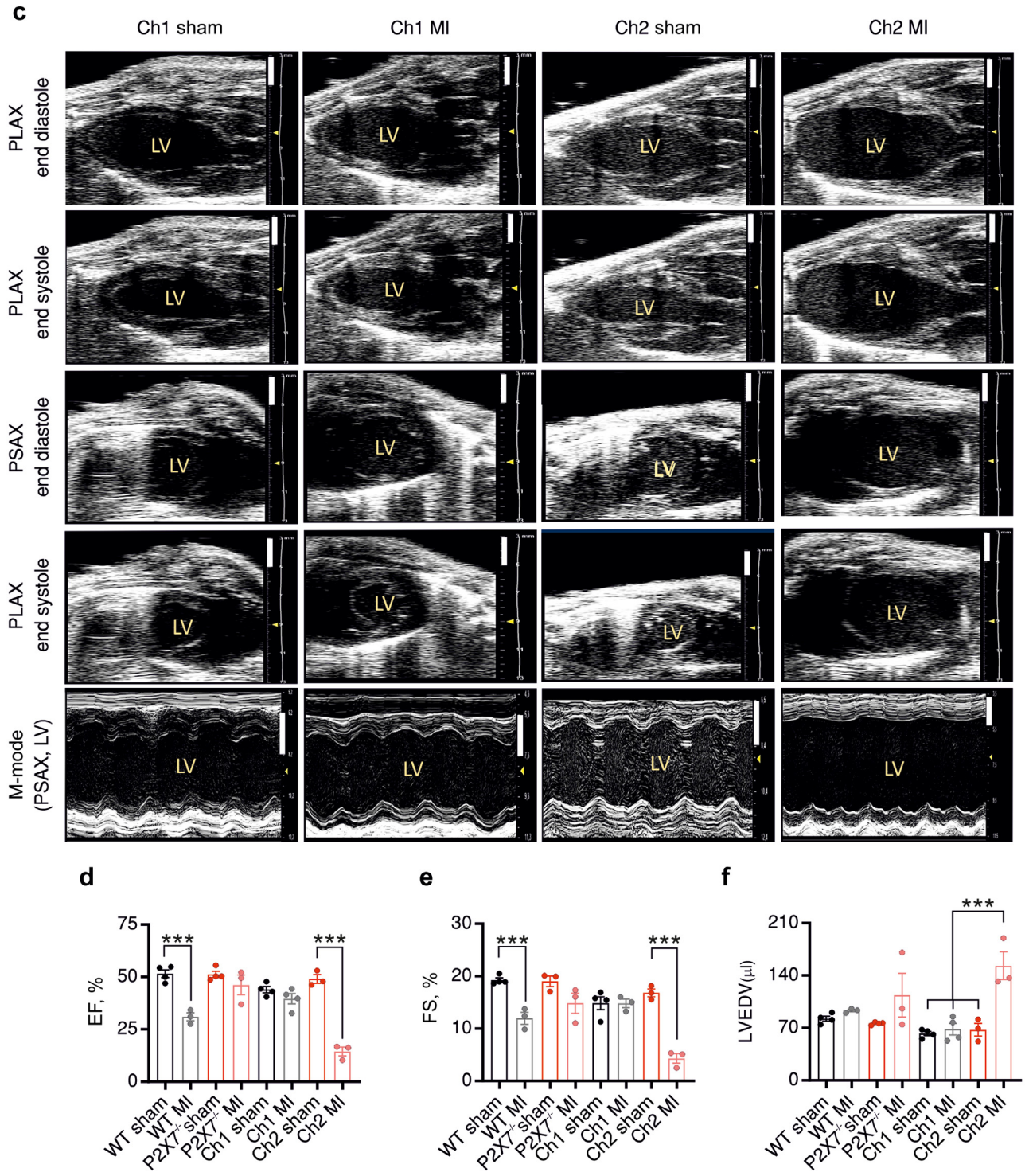

Figure 7 | (Continued) (**d**) Average ± SEM of ejection fraction (EF%), (**e**) left ventricular (LV) fractional shortening (FS%), and (**f**) LV endocardial diastolic volume (LVEDV), as quantified from measurements done as in (**b,c**). BM, bone marrow; Ch, chimera. To optimize viewing of this image, please see the online version of this article at www.kidney-international.org.

Here, we identify a novel facet of immunomodulation by P2X7. Although deletion of P2X7 abrogates the release of the inflammatory IL-1α/β, simultaneously P2X7 deletion facilitates surface accumulation of the adhesion molecule IL-1α on immune cells and promotes migration, thus potentially tissue infiltration[7] and thereby playing a dual immunomodulatory role. Noteworthy is that we observed significantly higher migration efficiency of P2X7$^{-/-}$ (Figure 2i and k) despite a

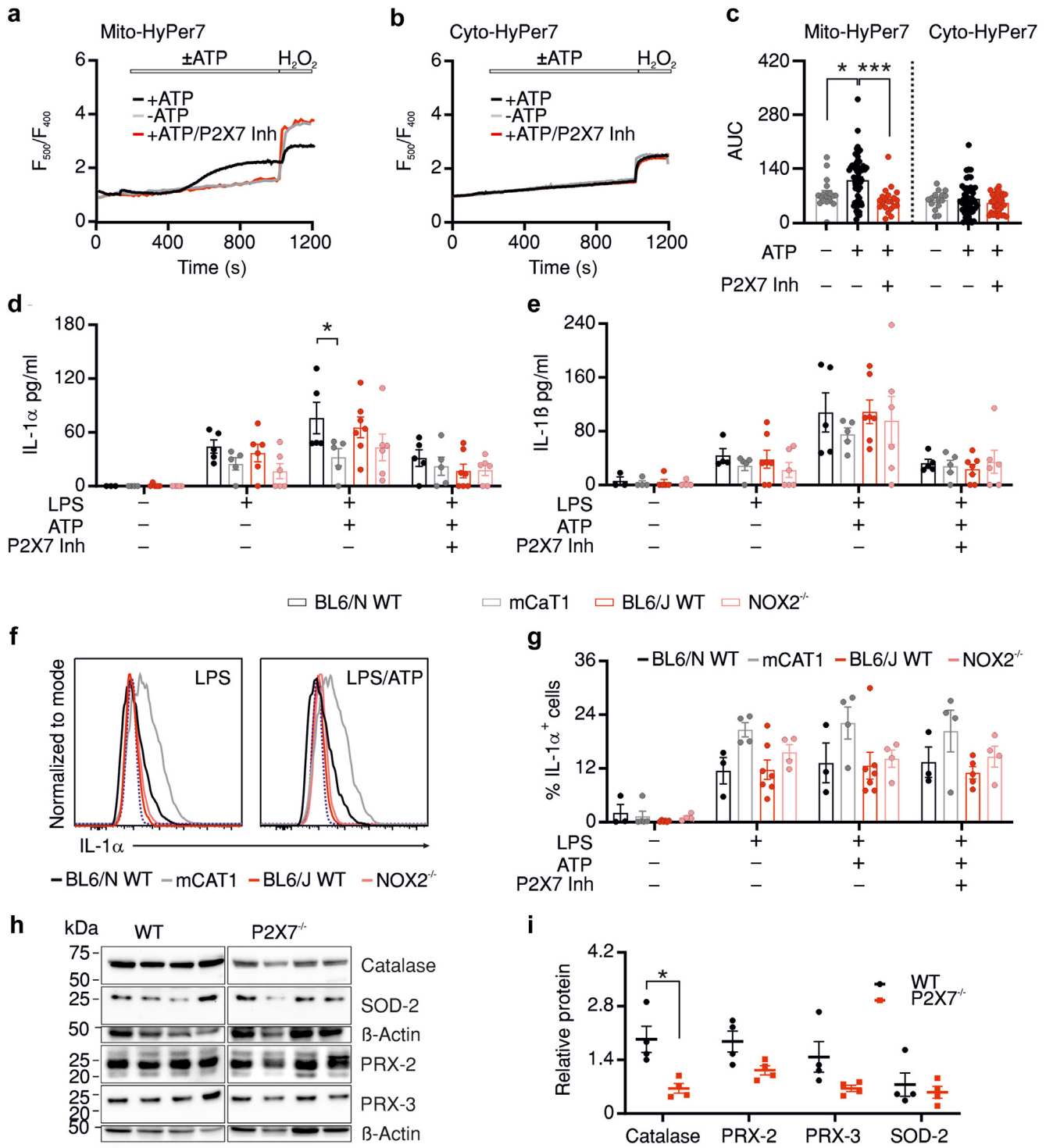

Figure 8 | Mitochondrial reactive oxygen species (ROS) are necessary for regulation of interleukin (IL)-1α secretion by P2X7. (**a,b**) Traces depicting averages of single experiments showing H_2O_2 production over time in human monocyte cell line (U937) expressing (**a**) mitochondrial (Mito-HyPer7) or (**b**) cytosolic (Cyto-Hyper7) H_2O_2 sensor on application of adenosine triphosphate (ATP)–free (gray), or ATP-containing (2 mM) buffer without (black) or with (red) preincubation (30 minutes) with P2X7 inhibitor (A804598; 100 μM). The 1 mM H_2O_2 was applied at the end of the measurement as positive control. (**c**) Bar graphs showing average area under the ATP response curve (AUC) of cells measured in (**a,b**). Analysis shows average ± SEM of 3 independent transfections, with 25 to 45 cells depicted with single dots. (**d,e**) Enzyme-linked immunosorbent assay measurements showing released (**d**) IL-1α or (**e**) IL-1β by bone marrow–derived macrophages (BMDMs) isolated from the indicated mouse lines. Cells were untreated, primed with lipopolysaccharide (LPS), or treated with LPS then ATP with or without preincubation (30 minutes) with P2X7 blocker (A804598; 100 μM), n = 3 to 6 mice/group. (**f**) Representative flow cytometry analysis and (**g**) quantification of surface expression of IL-1α on BMDMs isolated from the indicated mouse lines measured in (**d,e**). (**h**) Western blot images and (**i**) quantification showing analysis of the indicated cytosolic (catalase and peroxiredoxin-2 [PRX-2]) (continued)

decreased wound healing efficiency. The difference in the outcome of the 2 migration assays can be potentially explained by the retention of WT by cytokine gradient lacking in P2X7$^{-/-}$ BMDMs, with such gradient playing a role in the transwell but not the wound healing assay. Alternative explanation is a reduced proliferative capacity on P2X7 deletion.[44,45] This finding together with the higher expression of adhesion proteins in cardiac compared with kidney endothelial cells[46] may explain why P2X7 deletion reduces immune cell infiltration of injured kidneys but not the hearts.

Our study aimed to thoroughly characterize Ca^{2+} signaling profile alterations accompanying the development of kidney or cardiac disease models. Inflammasome activation,[47] phagocytosis,[48] and upregulation of CD80 and CD86[49,50] are Ca^{2+} dependent in monocytes and macrophages. Although macrophages exhibit functional SOCE, genetic ablation of the stromal interaction molecule (STIM) does not abolish their proinflammatory potential.[51] Instead, macrophages rely on P2X4- and P2X7-mediated Ca^{2+} influx for activation and signal propagation.[52] High AD resulted in reduced SOCE in the corresponding BMDMs, although this was P2X7 independent. This might be explained by high adenine-induced upregulation of integrin-linked kinase, which, in turn, inhibits glycogen synthase kinase-3 activity, thus reducing SOCE.[53–55] Inducing cardiac injury, on the other hand, was associated with an increased SOCE in BMDMs, which might be caused by the increased activity of glycogen synthase kinase-3, as observed by Wang *et al.*[56] In contrast, ATP-induced Ca^{2+} influx was consistently reduced in P2X7$^{-/-}$ compared with WT BMDMs, which together with the abolished cytokine secretion, support that P2X7 is the more physiologically relevant Ca^{2+} influx pathway for regulating proinflammatory functions of macrophages in CKD and CVD, as suggested by our Ca^{2+} profiling experiments of human cells. Noteworthy is that ATP-induced Ca^{2+} influx was reduced in LPS primed human monocytes and WT BMDMs concomitant to upregulation of P2X4 but not P2X7, in line with observations in microglia.[28] The debate whether, in cells expressing both subunits, P2X4 and P2X7 form true heteromultimeric channels with distinct properties is yet unresolved.[57–59] Our findings, however, suggest that higher levels of P2X4 inhibit P2X7-mediated Ca^{2+} influx, in agreement with current measurements by Casas-Pruneda *et al.* in cells transfected with different ratios of DNA encoding both subunits.[60] Moreover, P2X7-mediated Ca^{2+} influx can be altered by mechanisms regulating membrane trafficking and internalization of P2X7, such as posttranslational modification via phosphorylation, palmitoylation, or glycosylation of the C-terminus or the ectodomain of the protein (reviewed previously[61]). It remains elusive how these mechanisms are differentially regulated in immune cells versus nonhematopoietic cells and whether LAD ligation induces differences that potentially underlie the reduced ATP-induced Ca^{2+} responses in BMDMs derived from chimeric mice (Figure 6f) but not from WT mice subjected to the same intervention in Figure 4f or Figure 5f.

Our findings demonstrate that genetic ablation of P2X7 resulted in protection against AD-induced kidney infiltration by immune cell and upregulation of surface IL-1α but without beneficial effect on kidney function (Supplementary Figure S2G and H). These findings are in agreement with a recent study performed in rats[62] that, similar to our study, used global knockout approach in the kidney injury model. On the other hand, numerous studies support a crucial role of P2X7 in mediating cardiovascular diseases and show beneficial effects of P2X7 deletion (reviewed previously[63]). Mainly, these studies are based on global genetic ablation of P2X7; thus, we were unable to address whether the role of P2X7 was more prominent in immune cells or cardiomyocytes. Similarly, to our knowledge, to date only 2 other studies addressed the question of role of P2X7 on hematopoietic or nonhematopoietic cells in the context of kidney and cardiac diseases, both using kidney ischemia-reperfusion injury model. Our findings are in agreement with findings of Koo *et al.*, who suggest a more important role of P2X7 on the immune cells,[64] whereas findings of Qian *et al.* point to an important role of P2X7 on nonhematopoietic tissues.[65] Although not using chimeric but global knockout mice, Raggi *et al.* highlighted the role of P2X7-mediated inflammation in cardiac injury but also suggest that P2X7 might have a protective role in the heart because global P2X7$^{-/-}$ mice showed high-fat diet–induced myocardial hypertrophy and diastolic dysfunction.[66] We observed in mice with MI a similar tendency to numerically increased LV posterior wall thickness in P2X7$^{-/-}$ and even more so in Ch1 but not in Ch2. Thus, depending on the pathologic setting, P2X7 seems to play differential roles in immune cells and cardiomyocytes and might influence their interaction. Our results highlight that the presence of P2X7 on immune cells is essential to induce deleterious cardiac remodeling following MI also in absence of P2X7 in cardiomyocytes (Ch2). Further studies are needed to explore the mechanisms of how P2X7-expressing immune cells induce cardiac remodeling and to identify potential therapeutic strategies to treat or prevent cardiac injury, especially in patients with CKD.

Mechanistically, we present evidence that P2X7-induced mitochondrial ROS production is Ca^{2+} dependent and is essential for regulating IL-1α release. Signaling through P2X7 has been suggested to induce NOX2-dependent ROS production in microglia, astrocytes, and submandibular glands.[67–69]

Figure 8 | (continued) and mitochondrial (peroxireduxin-3 and superoxide dismutase 2 [SOD-2]) ROS-related proteins in kidney tissue lysates obtained from 4 mice either wild-type (WT; black) or P2X7$^{-/-}$ (red). Asterisks indicate significance at $^{*}P < 0.05$, $^{**}P < 0.01$, and $^{***}P < 0.001$. mCAT, mitochondrial catalase; NOX2, reduced nicotinamide adenine dinucleotide phosphate–oxidase 2. To optimize viewing of this image, please see the online version of this article at www.kidney-international.org.

Moore and MacKenzie used NOX2$^{-/-}$ derived BMDMs and concluded that ATP induces ROS in a NOX2-dependent manner based on the unaltered ethidium bromide permeability.[67] Although we cannot exclude that NOX2 is in part involved in P2X7-induced ROS production, our compartment-specific H_2O_2 measurements together with the reduction of IL-1α release in mitochondrial catalase mice strongly suggest that mitochondrial ROS together with P2X7-mediated Ca^{2+} influx regulate inflammation. Furthermore, our findings are supported by the unchanged activation of NLPR3 inflammasome in human and murine cells deficient for NOX1-4.[70,71]

Although our study emphasizes the role of P2X7 in regulating CKD-associated inflammation, we do not exclude that P2X4 contributes to disease progression. We show that similar to P2X7, P2X4 is upregulated in CKD monocytes. However, inhibition of P2X4 failed to induce significant reduction of secreted proinflammatory cytokines, supporting the stronger relevance of P2X7 in context of CKD. Nevertheless, our Ca^{2+} measurements and expression analyses of both receptors in inflammatory conditions indicate that P2X4 might indirectly influence the immunomodulatory effects of P2X7.

The fractions of immune cells infiltrating injured hearts or kidneys in our animal models were too low to allow isolation of adequate numbers of viable cells to perform our functional analyses. Our study relied, therefore, on investigating BMDMs. Besides being a time and cost-effective cellular model, BMDMs have been shown to play a crucial role in shaping the outcome of kidney injury[72] and cardiac infarction.[73,74] In addition, using the limited yield of tissue-resident cells, we show that heart-resident macrophages recapitulate P2X7-deficient BMDMs and circulating monocytes in terms of accumulating surface IL-1α (Supplementary Figure S6). Nonetheless, we acknowledge this limitation of our study and propose further investigations with single-cell multiomic approaches to explore differences in variable immune cell populations, beyond the populations that we addressed, as well as to identify P2X7-dependent molecular players inducing the differences we observed in susceptibility of heart and kidney tissues to cellular infiltration. Moreover, future studies are required to unravel P2X7-dependent (non-) immunomodulatory effects involved in cardiac remodeling.

In conclusion, by showing the dual-immunomodulatory role of P2X7, our study provides potential explanation of the controversial outcome regarding protective effects of P2X7 deletion while identifying P2X7 as a crucial regulator of chronic inflammation. Moreover, our findings highlight the importance of further studies to understand the clinical implications of P2X7 antagonists in cell adhesion and immune cell infiltration, in addition to altered antagonistic functions by P2X7 mutations, polymorphisms, or splicing events that may also underlie the variability of the outcome of translational studies using P2X7 antagonists in CKD.

DISCLOSURE

HN is founding shareholder of AMICARE Development GmbH; and MB is a member of the advisory boards for Amgen, Bayer, Boehringer Ingelheim, Cytokinetics, Medtronic, Novartis, Pfizer, ReCor, Servier, and Vifor. All the other authors declared no competing interests.

DATA STATEMENT

The current work does not contain big data sets or self-designed algorithms. The authors declare that all data supporting the findings of this study are available within the article. The authors will share any detailed information about any of the animal models or analytical procedures with anyone who wishes to use these models or procedures in their research. The appropriate authors to contact for various aspects of the research are MA, JF, PJ, EB, and DA.

ACKNOWLEDGMENTS

We thank Dr. Eichler (Clinical Hemostaseology and Transfusion Medicine) and Dr. Schwarz for support with blood samples; Dr. Hoth and Dr. Laschke for support with equipment and animal housing; and Mrs. Janku, Förderer, and Noll and Mr. Hauck for technical assistance. This work was supported by the Deutsche Forschungsgemeinschaft (DFG) project ID 322900939 to HN, SS, MB, MH, BAN, LPR, and TSp; the DFG project SFB1027 to BAN; and Saarland University, HOMFOR excellent to DA. The DFG funded the FACSverse (GZ: INST 256/423-1 FUGG), Cell Discoverer7 (GZ: INST 256/555-1 FUGG), and Cell Observer (GZ: INST 256/256-1 FUGG).

AUTHOR CONTRIBUTIONS

All authors conceptualized the study and edited the manuscript; EB performed animal procedures; MA, JF, PJ, EB, TSa, S-RS, AS, and DA performed experiments and data analysis; JE, CM, and LPR provided mice; SS, BAN, LPR, MB, MH, TSp, and DA secured funding and resources; and DA wrote the first draft of the manuscript.

Supplementary material is available online at www.kidney-international.org.

REFERENCES

1. Wong LY, Liew AST, Weng WT, et al. Projecting the burden of chronic kidney disease in a developed country and its implications on public health. *Int J Nephrol*. 2018;2018:5196285.
2. McCullough KP, Morgenstern H, Saran R, et al. Projecting ESRD incidence and prevalence in the United States through 2030. *J Am Soc Nephrol*. 2019;30:127–135.
3. George C, Echouffo-Tcheugui JB, Jaar BG, et al. The need for screening, early diagnosis, and prediction of chronic kidney disease in people with diabetes in low- and middle-income countries-a review of the current literature. *BMC Med*. 2022;20:247.
4. Murphy D, McCulloch CE, Lin F, et al. Trends in prevalence of chronic kidney disease in the United States. *Ann Intern Med*. 2016;165:473–481.
5. Gupta J, Mitra N, Kanetsky PA, et al. Association between albuminuria, kidney function, and inflammatory biomarker profile in CKD in CRIC. *Clin J Am Soc Nephrol*. 2012;7:1938–1946.
6. Cohen SD, Phillips TM, Khetpal P, et al. Cytokine patterns and survival in haemodialysis patients. *Nephrol Dial Transplant*. 2010;25:1239–1243.
7. Schunk SJ, Triem S, Schmit D, et al. Interleukin-1alpha Is a central regulator of leukocyte-endothelial adhesion in myocardial infarction and in chronic kidney disease. *Circulation*. 2021;144:893–908.
8. Chen BC, Chou CF, Lin WW. Pyrimidinoceptor-mediated potentiation of inducible nitric-oxide synthase induction in J774 macrophages: role of intracellular calcium. *J Biol Chem*. 1998;273:29754–29763.
9. Watanabe N, Suzuki J, Kobayashi Y. Role of calcium in tumor necrosis factor-alpha production by activated macrophages. *J Biochem*. 1996;120:1190–1195.
10. Schroder K, Zhou R, Tschopp J. The NLRP3 inflammasome: a sensor for metabolic danger? *Science*. 2010;327:296–300.
11. Gallin EK. Calcium- and voltage-activated potassium channels in human macrophages. *Biophys J*. 1984;46:821–825.

12. Knowles H, Li Y, Perraud AL. The TRPM2 ion channel, an oxidative stress and metabolic sensor regulating innate immunity and inflammation. *Immunol Res*. 2013;55:241–248.
13. Feske S, Skolnik EY, Prakriya M. Ion channels and transporters in lymphocyte function and immunity. *Nat Rev Immunol*. 2012;12:532–547.
14. Lajdova I, Oksa A, Chorvat D Jr, et al. Purinergic P2X7 receptors participate in disturbed intracellular calcium homeostasis in peripheral blood mononuclear cells of patients with chronic kidney disease. *Kidney Blood Press Res*. 2012;35:48–57.
15. Ainscough JS, Gerberick GF, Kimber I, et al. Interleukin-1beta processing is dependent on a calcium-mediated interaction with calmodulin. *J Biol Chem*. 2015;290:31151–31161.
16. Zewinger S, Reiser J, Jankowski V, et al. Apolipoprotein C3 induces inflammation and organ damage by alternative inflammasome activation. *Nat Immunol*. 2020;21:30–41.
17. Kilkenny C, Browne WJ, Cuthill IC, et al. Improving bioscience research reporting: the ARRIVE guidelines for reporting animal research. *PLoS Biol*. 2010;8:e1000412.
18. Erratum: Kidney Disease: Improving Global Outcomes (KDIGO) CKD-MBD Update Work Group. KDIGO 2017 Clinical Practice Guideline Update for the Diagnosis, Evaluation, Prevention, and Treatment of Chronic Kidney Disease-Mineral and Bone Disorder (CKD-MBD). *Kidney Int Suppl*. 2017;7:1–59. *Kidney Int Suppl (2011)*. 2017;7:e1.
19. Lameire NH, Levin A, Kellum JA, et al. Harmonizing acute and chronic kidney disease definition and classification: report of a Kidney Disease: Improving Global Outcomes (KDIGO) Consensus Conference. *Kidney Int*. 2021;100:516–526.
20. Roos J, DiGregorio PJ, Yeromin AV, et al. STIM1, an essential and conserved component of store-operated Ca2+ channel function. *J Cell Biol*. 2005;169:435–445.
21. Vig M, Peinelt C, Beck A, et al. CRACM1 is a plasma membrane protein essential for store-operated Ca2+ entry. *Science*. 2006;312:1220–1223.
22. Yamamoto S, Shimizu S, Kiyonaka S, et al. TRPM2-mediated Ca2+influx induces chemokine production in monocytes that aggravates inflammatory neutrophil infiltration. *Nat Med*. 2008;14:738–747.
23. Graham S, Yuan JP, Ma R. Canonical transient receptor potential channels in diabetes. *Exp Biol Med (Maywood)*. 2012;237:111–118.
24. Miller BA. The role of TRP channels in oxidative stress-induced cell death. *J Membr Biol*. 2006;209:31–41.
25. Ward JR, West PW, Ariaans MP, et al. Temporal interleukin-1beta secretion from primary human peripheral blood monocytes by P2X7-independent and P2X7-dependent mechanisms. *J Biol Chem*. 2010;285:23147–23158.
26. Luz HL, Reichel M, Unwin RJ, et al. P2X7 receptor stimulation is not required for oxalate crystal-induced kidney injury. *Sci Rep*. 2019;9:20086.
27. Taylor SR, Turner CM, Elliott JI, et al. P2X7 deficiency attenuates renal injury in experimental glomerulonephritis. *J Am Soc Nephrol*. 2009;20:1275–1281.
28. Trang M, Schmalzing G, Muller CE, et al. Dissection of P2X4 and P2X7 receptor current components in BV-2 microglia. *Int J Mol Sci*. 2020;21:8489.
29. Jankowski J, Floege J, Fliser D, et al. Cardiovascular disease in chronic kidney disease: pathophysiological insights and therapeutic options. *Circulation*. 2021;143:1157–1172.
30. Solle M, Labasi J, Perregaux DG, et al. Altered cytokine production in mice lacking P2X(7) receptors. *J Biol Chem*. 2001;276:125–132.
31. Munoz FM, Patel PA, Gao X, et al. Reactive oxygen species play a role in P2X7 receptor-mediated IL-6 production in spinal astrocytes. *Purinergic Signal*. 2020;16:97–107.
32. Fontanils U, Seil M, Pochet S, et al. Stimulation by P2X(7) receptors of calcium-dependent production of reactive oxygen species (ROS) in rat submandibular glands. *Biochim Biophys Acta*. 2010;1800:1183–1191.
33. Hewinson J, Moore SF, Glover C, et al. A key role for redox signaling in rapid P2X7 receptor-induced IL-1 beta processing in human monocytes. *J Immunol*. 2008;180:8410–8420.
34. Pollock JD, Williams DA, Gifford MA, et al. Mouse model of X-linked chronic granulomatous disease, an inherited defect in phagocyte superoxide production. *Nat Genet*. 1995;9:202–209.
35. Schriner SE, Linford NJ, Martin GM, et al. Extension of murine life span by overexpression of catalase targeted to mitochondria. *Science*. 2005;308:1909–1911.
36. Glorieux C, Calderon PB. Catalase, a remarkable enzyme: targeting the oldest antioxidant enzyme to find a new cancer treatment approach. *Biol Chem*. 2017;398:1095–1108.
37. Cao Z, Lindsay JG. The peroxiredoxin family: an unfolding story. *Subcell Biochem*. 2017;83:127–147.
38. Huang Z, Xie N, Illes P, et al. From purines to purinergic signalling: molecular functions and human diseases. *Signal Transduct Target Ther*. 2021;6:162.
39. Menzies RI, Tam FW, Unwin RJ, et al. Purinergic signaling in kidney disease. *Kidney Int*. 2017;91:315–323.
40. Zhang WJ. Effect of P2X purinergic receptors in tumor progression and as a potential target for anti-tumor therapy. *Purinergic Signal*. 2021;17:151–162.
41. Yan Y, Bai J, Zhou X, et al. P2X7 receptor inhibition protects against ischemic acute kidney injury in mice. *Am J Physiol Cell Physiol*. 2015;308:C463–C472.
42. Keystone EC, Wang MM, Layton M, et al. Clinical evaluation of the efficacy of the P2X7 purinergic receptor antagonist AZD9056 on the signs and symptoms of rheumatoid arthritis in patients with active disease despite treatment with methotrexate or sulphasalazine. *Ann Rheum Dis*. 2012;71:1630–1635.
43. Eltom S, Stevenson CS, Rastrick J, et al. P2X7 receptor and caspase 1 activation are central to airway inflammation observed after exposure to tobacco smoke. *PLoS One*. 2011;6:e24097.
44. Ghazi K, Deng-Pichon U, Warnet JM, et al. Hyaluronan fragments improve wound healing on *in vitro* cutaneous model through P2X7 purinoreceptor basal activation: role of molecular weight. *PLoS One*. 2012;7:e48351.
45. Leeson HC, Kasherman MA, Chan-Ling T, et al. P2X7 receptors regulate phagocytosis and proliferation in adult hippocampal and SVZ neural progenitor cells: implications for inflammation in neurogenesis. *Stem Cells*. 2018;36:1764–1777.
46. Marcu R, Choi YJ, Xue J, et al. Human organ-specific endothelial cell heterogeneity. *iScience*. 2018;4:20–35.
47. Murakami T, Ockinger J, Yu J, et al. Critical role for calcium mobilization in activation of the NLRP3 inflammasome. *Proc Natl Acad Sci U S A*. 2012;109:11282–11287.
48. Nunes P, Demaurex N. The role of calcium signaling in phagocytosis. *J Leukoc Biol*. 2010;88:57–68.
49. Wilhelm K, Ganesan J, Muller T, et al. Graft-versus-host disease is enhanced by extracellular ATP activating P2X7R. *Nat Med*. 2010;16:1434–1438.
50. Pinto BF, Medeiros NI, Teixeira-Carvalho A, et al. CD86 expression by monocytes influences an immunomodulatory profile in asymptomatic patients with chronic Chagas disease. *Front Immunol*. 2018;9:454.
51. Vaeth M, Zee I, Concepcion AR, et al. Ca2+ signaling but not store-operated Ca2+ entry is required for the function of macrophages and dendritic cells. *J Immunol*. 2015;195:1202–1217.
52. Zumerle S, Cali B, Munari F, et al. Intercellular calcium signaling induced by ATP potentiates macrophage phagocytosis. *Cell Rep*. 2019;27:1–10.e14.
53. Schmid E, Yan J, Nurbaeva MK, et al. Decreased store operated Ca2+ entry in dendritic cells isolated from mice expressing PKB/SGK-resistant GSK3. *PLoS One*. 2014;9:e88637.
54. de Frutos S, Luengo A, Garcia-Jerez A, et al. Chronic kidney disease induced by an adenine rich diet upregulates integrin linked kinase (ILK) and its depletion prevents the disease progression. *Biochim Biophys Acta Mol Basis Dis*. 2019;1865:1284–1297.
55. Wu C, Dedhar S. Integrin-linked kinase (ILK) and its interactors: a new paradigm for the coupling of extracellular matrix to actin cytoskeleton and signaling complexes. *J Cell Biol*. 2001;155:505–510.
56. Wang SH, Cui LG, Su XL, et al. GSK-3beta-mediated activation of NLRP3 inflammasome leads to pyroptosis and apoptosis of rat cardiomyocytes and fibroblasts. *Eur J Pharmacol*. 2022;920:174830.
57. Craigie E, Birch RE, Unwin RJ, et al. The relationship between P2X4 and P2X7: a physiologically important interaction? *Front Physiol*. 2013;4:216.
58. Antonio LS, Stewart AP, Xu XJ, et al. P2X4 receptors interact with both P2X2 and P2X7 receptors in the form of homotrimers. *Br J Pharmacol*. 2011;163:1069–1077.
59. Saul A, Hausmann R, Kless A, et al. Heteromeric assembly of P2X subunits. *Front Cell Neurosci*. 2013;7:250.
60. Casas-Pruneda G, Reyes JP, Perez-Flores G, et al. Functional interactions between P2X4 and P2X7 receptors from mouse salivary epithelia. *J Physiol*. 2009;587:2887–2901.
61. Sluyter R. The P2X7 receptor. *Adv Exp Med Biol*. 2017;1051:17–53.

62. Nespoux J, Monaghan MT, Jones NK, et al. P2X7 receptor knockout does not alter renal function or prevent angiotensin II-induced kidney injury in F344 rats. *Sci Rep*. 2024;14:9573.
63. Zhou J, Zhou Z, Liu X, et al. P2X7 receptor-mediated inflammation in cardiovascular disease. *Front Pharmacol*. 2021;12:654425.
64. Koo TY, Lee JG, Yan JJ, et al. The P2X7 receptor antagonist, oxidized adenosine triphosphate, ameliorates renal ischemia-reperfusion injury by expansion of regulatory T cells. *Kidney Int*. 2017;92:415–431.
65. Qian Y, Qian C, Xie K, et al. P2X7 receptor signaling promotes inflammation in renal parenchymal cells suffering from ischemia-reperfusion injury. *Cell Death Dis*. 2021;12:132.
66. Raggi F, Rossi C, Faita F, et al. P2X7 receptor and heart function in a mouse model of systemic inflammation due to high fat diet. *J Inflamm Res*. 2022;15:2425–2439.
67. Moore SF, MacKenzie AB. NADPH oxidase NOX2 mediates rapid cellular oxidation following ATP stimulation of endotoxin-primed macrophages. *J Immunol*. 2009;183:3302–3308.
68. Noguchi T, Ishii K, Fukutomi H, et al. Requirement of reactive oxygen species-dependent activation of ASK1-p38 MAPK pathway for extracellular ATP-induced apoptosis in macrophage. *J Biol Chem*. 2008;283:7657–7665.
69. Parvathenani LK, Tertyshnikova S, Greco CR, et al. P2X7 mediates superoxide production in primary microglia and is up-regulated in a transgenic mouse model of Alzheimer's disease. *J Biol Chem*. 2003;278:13309–13317.
70. van Bruggen R, Koker MY, Jansen M, et al. Human NLRP3 inflammasome activation is Nox1-4 independent. *Blood*. 2010;115:5398–5400.
71. Guerra Martinez C. P2X7 receptor in cardiovascular disease: the heart side. *Clin Exp Pharmacol Physiol*. 2019;46:513–526.
72. Cao Q, Wang Y, Zheng D, et al. Failed renoprotection by alternatively activated bone marrow macrophages is due to a proliferation-dependent phenotype switch *in vivo*. *Kidney Int*. 2014;85:794–806.
73. Chen B, Luo L, Wei X, et al. M1 bone marrow-derived macrophage-derived extracellular vesicles inhibit angiogenesis and myocardial regeneration following myocardial infarction via the MALAT1/microRNA-25-3p/CDC42 axis. *Oxid Med Cell Longev*. 2021;2021:9959746.
74. Nahrendorf M, Swirski FK, Aikawa E, et al. The healing myocardium sequentially mobilizes two monocyte subsets with divergent and complementary functions. *J Exp Med*. 2007;204:3037–3047.